Mechanism-Based Inhibition of Thymidylate Synthase by 5-(Trifluoromethyl)-2′-deoxyuridine 5′-Monophosphate†

Jens W. Eckstein,‡,§ Paul G. Foster,|| Janet Finer-Moore,⊥ Yusuke Wataya,‡,# and Daniel V. Santi*,‡,⊥

Department of Pharmaceutical Chemistry, Graduate Group in Biophysics, and Department of Biochemistry and Biophysics, University of California, San Francisco, California 94143-0448

Received July 21, 1994; Revised Manuscript Received September 26, 1994®

ABSTRACT: Thymidylate synthase (TS) from *Lactobacillus casei* is inhibited by 5-(trifluoromethyl)-2′-deoxyuridine 5′-monophosphate (CF_3dUMP). CF_3dUMP binds to the active site of TS in the absence of 5,10-methylenetetrahydrofolate, and attack of the catalytic nucleophile cysteine 198 at C_6 of the pyrimidine leads to activation of the trifluoromethyl group and release of fluoride ion. Subsequently, the activated heterocycle reacts with a nucleophile of the enzyme to form a moderately stable covalent complex. Proteolytic digestion of TS treated with [2′-^{3}H]CF_3dUMP, followed by sequencing of the labeled peptides, revealed that tyrosine 146 and cysteine 198 are covalently bound to the inhibitor in the enzyme−inhibitor complex. The presence of dithiothreitol (DTT) or β-mercaptoethanol resulted in the breakdown of the covalent complex, and products from the breakdown of the complex were isolated and characterized. The three-dimensional structure of the enzyme−inhibitor complex was determined by X-ray crystallography, clearly demonstrating covalent attachment of the nucleotide to tyrosine 146. A chemical reaction mechanism for the inhibition of TS by CF_3dUMP is presented that is consistent with the kinetic, biochemical, and structural results.

Thymidylate synthase (TS,[1] EC 2.1.1.45) catalyzes the reductive methylation of 2′-deoxyuridine 5′-monophosphate (dUMP) to thymidine 5′-monophosphate (dTMP) with the concomitant conversion of CH_2H_4folate to H_2folate. Since TS is the last enzyme in the sole *de novo* pathway for dTMP synthesis, it has been a important target for antineoplastic agents. Considerable efforts have been devoted to the discovery and understanding of inhibitors of this enzyme. As early as 1965, it was reported that 5-(trifluoromethyl)-2′-deoxyuridine 5′-monophosphate (CF_3dUMP) was an irreversible inhibitor of TS in extracts of Ehrlich ascites cells (Reyes & Heidelberger, 1965). 5-(Trifluoromethyl)-2′-deoxyuridine (CF_3dUrd), a metabolic precursor of CF_3dUMP, is a potent inhibitor of cell growth (Umeda & Heidelberger, 1968) and has been tested extensively both as a chemotherapeutic agent and an antiviral agent (Heidelberger & King, 1979). Currently, CF_3dUrd serves as a topical agent to treat Herpes keratitis (Carmine et al., 1982). Although the inhibition of TS by CF_3dUMP has been recognized for almost 3 decades and various elements of the interaction have been proposed, the mechanism of inhibition remains to be elucidated.

A key feature of the irreversible inhibition of TS by CF_3dUMP is the cleavage of its carbon−fluorine bonds. Although carbon−fluorine bonds generally are quite strong, β-elimination of a fluoride ion may occur when a negative charge is generated on the carbon adjacent to a C−F bond (Sakai & Santi, 1973). The resultant olefinic carbon may undergo attack by a nucleophile, and if additional fluorine atoms are attached, successive addition−elimination reactions result in the cleavage of all C−F bonds. In model studies, attack of a nucleophile at C_6 of 1-substituted 5-(trifluoromethyl)uracils activates the trifluoromethyl group and leads to carbon−fluorine bond cleavage (Santi & Sakai, 1971). The loss of the first fluoride ion produces an exocyclic difluoromethylene carbon that is susceptible to the addition of a second nucleophile (Scheme 1) (Santi & Sakai, 1971; Wataya et al., 1987) and ultimately an acyl derivative of that nucleophile. Under basic aqueous conditions, a series of addition−elimination reactions results in 5-carboxyuracil, which is the major metabolite of 4-(trifluoromethyl)uracil and CF_3dUrd degradation *in vivo* (Heidelberger et al., 1965).

For the inhibition of TS by CF_3dUMP, Santi and Sakai proposed that a nucleophilic catalyst of the TS reaction (Cys 198) in the active site functions as the activating nucleophile (Santi & Sakai, 1971). Addition of this nucleophile to the C_6 of CF_3dUMP results in the formation of an exocyclic difluoromethylene intermediate, which could then be attacked by a nearby second nucleophilic residue, irreversibly acylating the enzyme.

With crystal structures of TS available, we revisited questions on the mechanism of CF_3dUMP inhibition; we asked whether earlier proposals were viable in the context of the structure and attempted to identify the putative residue of TS that was covalently modified. Using the *Lactobacillus casei* TS−dUMP crystal structure, we modeled a TS−CF_3dUMP complex. Analysis of this model indicated that no nucleophilic residues of the enzyme were within covalent-bond-forming distance of the CF_3 moiety of CF_3dUMP, but

† This work was supported by U.S. Public Health Service Grants CA-14394 (D.V.S.) and CA-41323 (J.F.M.) from the National Institutes of Health. P.G.F. is supported by NIH Training Grant GM-08382-06.

* Author to whom correspondence should be addressed.

‡ Department of Pharmaceutical Chemistry.

§ Present address: Mitotix Inc., One Kendall Square, Cambridge, MA 02139.

|| Graduate Group in Biophysics.

⊥ Department of Biochemistry and Biophysics.

Present address: Faculty of Pharmaceutical Sciences, Okayama University, Tsushima, Okayama 700, Japan.

® Abstract published in *Advance ACS Abstracts,* November 15, 1994.

[1] Abbreviations: TS, thymidylate synthase; CF_3dUrd, 5-(trifluoromethy)-2′-deoxyuridine; CF_3dUMP, 5-(trifluoromethyl)-2′-deoxyuridine 5′-monophosphate; dUMP, 2′-deoxyuridine 5′-monophosphate; dTMP, thymidine 5′-monophosphate; CH_2H_4folate, 5,10-methylenetetrahydrofolate; *N*-[tris(hydroxymethyl)methyl]-2-aminoethanesulfonic acid; LEP, lysylendopeptidase; DTT, dithiothreitol; rms, root mean square.

0006-2960/94/0433-15086$04.50/0 © 1994 American Chemical Society

Scheme 1

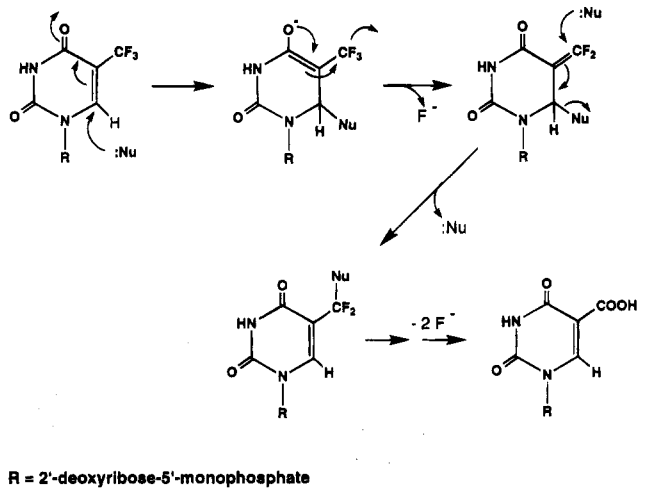

that His 199 and Tyr 146 were the most likely candidates for the acylated nucleophiles, with distances from the CF_3 group of 4.5 and 4.3 Å, respectively. In the present work, we describe experiments that verify old and uncover new aspects of the mechanism of TS inhibition by CF_3dUMP and identify the acylated residue of TS as Tyr 146.

MATERIALS AND METHODS

Materials. CF_3dUrd was purchased from Sigma and converted to CF_3dUMP with wheat germ phosphotransferase, as described for nucleotide monophosphate production (Prasher et al., 1982). CF_3dUrd and CF_3dUMP were purified with HPLC system A (see the following). [2′-^{3}H]CF_3dU (11 Ci/mmol) was purchased from Moravek (Brea, CA). Lysylendopeptidase (LEP) was purchased from Wako. All other chemicals were bought from commercial sources and used without further purification. TS was purified by an automated purification system described previously (Kealey & Santi, 1992). TS activity was assessed by a spectrophotometric assay (Pogolotti et al., 1986), and purity was monitored by 12% SDS−PAGE stained with Coomassie Blue R250 (Laemmli, 1970). Protein concentrations were estimated according to Bradford (1976), and concentrations of pure enzyme were determined by using an ϵ_{278} of 1.25×10^5 cm^{-1} M^{-1} for TS dimer (Greene et al., 1993). Enzyme concentrations in all TS−CF_3dUMP reactions are for TS monomer, except where noted. The standard TES buffer consisted of 50 mM TES, 25 mM $MgCl_2$, 6.5 mM HCHO, and 1 mM EDTA and was used for all experiments except where noted. Amino acid sequencing was carried out at the Biomolecular Resource Center, UCSF. Peptides and reaction products were analyzed using electrospray mass spectroscopy at the UCSF Mass Spectroscopy Facility.

HPLC. All chromatography was carried out at room temperature. System A: Rainin HPXL solvent delivery system with Dynamax UV-1 detector; Altex Ultrasphere-IP column 5 μm, 4.6 × 250 mm. Data acquisition and analysis were done using a Rainin software package operating on an Apple Macintosh computer. The following conditions were used: flow, 1 mL/min; injection, 25 min at 100% solvent A (5 mM KP_i, 5 mM tetrabutylammonium hydrogen sulfate, and 10% CH_3CN, pH 7), followed by a 10 min linear gradient to 60% solvent B (5 mM KP_i, 5 mM tetrabutylammonium hydrogen sulfate, and 60% CH_3CN, pH 7). System B: Hewlett-Packard Aminoquant 1090 Series II system connected to a Hewlett-Packard HPLC ChemStation, Brownlee Labs narrow bore C-8 RP300 column, 2.1 × 30 mm. The following conditions were used: flow, 200 μL/min; injection, 5 min wash with 100% solvent C (0.1% trifluoroacetic acid in water), followed by a 25 min linear gradient to 90% solvent B (70% CH_3CN and 0.1% trifluoroacetic acid/water). Absorbance was monitored at 215 nm on a Hewlett-Packard diode array detector. System C: Pharmacia HR10/10 fast desalting FPLC column; flow, 2 mL/min; mobile phase was water. System D: preparative Econosil RP18 column, 10 × 250 mm; flow, 1 mL/min; wash with solvent A (10 mM $NH_4^+HCOO^-$, pH 7.5) followed by a linear gradient of 10−60% solvent B (MeOH).

Degradation of the TS−CF_3dUMP Complex with DTT. A preformed complex containing 250 μM CF_3dUMP and 50 μM TS was treated with 30 mM DTT, and aliquots removed at various times were either diluted 60-fold into solutions for activity assay or filtered through a Sephadex G-25 superfine column (NAP-25 column, Pharmacia) to separate enzyme from free ligand prior to activity assay. Gel filtration chromatography was carried out at 4 °C in buffer containing 50 mM *N*-methylmorpholine, 25 mM $MgCl_2$, and 1 mM EDTA (pH 7.4).

UV/Visible Spectroscopy. All spectra were recorded on a Hewlett-Packard 8452A diode array spectrophotometer. Difference spectra were obtained by subtracting the spectrum of enzyme from the total spectrum. Corrections were made for dilution and light scattering.

Filter Binding Assays. A reaction mixture containing 10 μM TS and 30 μM [2′-^{3}H]CF_3dUMP (158 Ci/mol) in TES buffer was incubated with and without 70 μM CH_2H_4folate; 25 μL aliquots (14 000 dpm) were removed over 90 min and applied to a nitrocellulose filter (BA-85, Schleicher and Schuell). The filter was washed and counted as previously described (Bruice & Santi, 1982).

Fluoride Ion Determinations. Fluoride ion release was measured using an Orion fluoride electrode (Model 94-09) and an Orion pH/millivolt meter (Model 611). The electrode was calibrated by serial dilution of a 0.1 M NaF standard solution (Orion). In all experiments, 1 1:1 TISAB (total ion strength adjustment buffer)/CDTA (*trans*-1,2-diaminocyclohexane-*N*,*N*,*N*′,*N*′-tetraacetic acid) solution (Orion) was used to adjust conductivity to 50 mS. ^{19}F NMR spectra were recorded at 282.3 MHz on a GE 300 NMR spectrometer, employing $CFCl_3$ as an external reference. The concentrations of TS and CF_3dUMP were 110 and 200 μM, respectively.

Peptide Mapping and Amino Acid Sequencing. A 350 μL reaction mixture containing 43 μM TS and 50 μM [2′-^{3}H]CF_3dUMP (171 Ci/mol) in TES buffer was incubated at room temperature for 90 min and then digested with 550 μL containing 0.2 unit of LEP in 5 M guanidine hydrochloride and 50 mM Tris-HCl (pH 8.9) for 30 h at 30 °C. The mixture was analyzed using HPLC system B. Amino acid sequences of HPLC-purified peptides were determined by Edman degradation, as previously described (Kealey & Santi, 1991). The phenylthiohydrantoin derivatives from each sequencing cycle were collected, and 40 μL aliquots were counted in 8 mL of Aquasol II/2 mL of H_2O on a Beckman LS 3801 liquid scintillation counter.

Isolation and Purification of Reaction Products. Method 1: A 1 mL reaction mixture containing 4 μM TS, 1.8 mM

[2′-^{3}H]CF_3dUMP (140 nCi/μmol), and 6 mM DTT in TES buffer was incubated at room temperature for 84 h. The mixture was applied to Whatman 3 mm chromatography paper (28 × 40 cm) and developed with isobutyric acid/0.5 NH_4OH (6:10, v/v), yielding two spots, product A and product B. The second band from the top (R_f = 0.43) was the main product. Method 2: A 4 mL reaction mixture containing 120 μM TS and 250 μM CF_3dUMP in TES buffer was incubated at room temperature for 1 h, followed by the addition of DTT to 20 mM with continued incubation at room temperature for 2 h. The enzyme was removed using a Centricon 30 concentrator (Amicon, 3 × 15 min at 3000g). The solution was evaporated *in vacuo*, redissolved in 5% MeOH/H_2O, and subjected to HPLC using system D, and products were identified by UV/vis spectra.

Autoradiography. A 1 mL reaction mixture containing 8.5 μM TS and 10 μM [2′-^{3}H]CF_3dUMP (600 μCi/μmol) in TES buffer was incubated for 40 min. The reaction mixture was analyzed by SDS−PAGE and prepared for autoradiography as described previously (Chamberlain, 1979).

Molecular Modeling. CF_3dUMP was modeled into the active site of the TS−dUMP binary complex (Finer-Moore et al., 1993) using QUANTA/CHARMm (Molecular Simulations, Inc., Waltham, MA) on a Silicon Graphics Personal Iris workstation. CF_3dUMP was placed into the active site by first superimposing it with bound dUMP. A bond was constructed between the sulfur of the active site cysteine and C_6 of CF_3dUMP, followed by a shift of the C_5−C_6 double bond to a C_5−C_7 double bond and removal of one fluoride ion from the trifluoromethyl group carbon C_7. The structure was energy minimized using the steepest descent algorithm followed by Adopted-Basis Newton Raphson minimization.

TS−CF_3dUMP Crystallization. Crystals of TS−CF_3dUMP complex were obtained as previously described for the *L. casei* TS−dUMP structure (Finer-Moore et al., 1993), except all solutions contained TES buffer (100 mM TES (pH 7.4) and 0.1 mM EDTA) in place of phosphate. Prior to crystallization, 13 mg/mL TS was dialyzed overnight against TES buffer and incubated for 30 min with 1 mM DTT. After the removal of exogenous DTT by gel filtration (NAP-5 column, Pharmacia), the protein fraction was mixed with CF_3dUMP and used for crystallization by hanging-drop vapor diffusion against TES buffer. Crystallization drops contained 10 mg/mL TS, 0.5 mM CF_3dUMP, and 1−2% saturated $(NH_4)_2SO_4$ in TES buffer.

X-ray Data Collection. Diffraction data from a single crystal of TS−CF_3dUMP were collected on a Fuji Image Plate (R-AxisIIC) using a 300 μm collimated beam of graphite-monochromated Cu Kα X-rays generated by a Rigaku rotating anode. Thirty data frames were collected, each covering a 2° oscillation range over 40 min, with a 2θ setting of 19° and a crystal to detector distance of 23.6 cm. The data were indexed and reduced using the R-AxisIIC automated programs (Higashi, 1990; Sato et al., 1992). Additional data from a second crystal were collected on a Siemens area detector, using a 300 μm collimated beam of graphite-monochromated Cu Kα X-rays generated by a Rigaku rotating anode. Oscillation widths were 0.2° in ω, and counting times were as high as 6 min/frame for the higher resolution data (2θ = 22°). The crystal to detector distance was 30 cm. These data were indexed and integrated using the program XDS (Kabsch, 1982) and then scaled and merged using the program Rotavata/Agrovata (CCP4, Daresbury England). The space group and unit cell dimensions were the same as those obtained from image plate data, and all reflections were later merged using a locally written program with Wilson scaling (D. A. Agard, personal communication). Statistics for the crystallographic data are given in Table 1.

Table 1: Crystallographic Data Statistics for TS−CF_3dUMP

X-ray detection	image plate	area detector
space group	$P6_122$	$P6_122$
resolution (Å)	∞−2.3	∞−2.6
total observations	43699	15737
unique reflections	14543	8117
$I/\sigma I$	5.35	8.55
R_{factor} (%)	11[a]	6.1[b]
completeness (%)	89	77

[a] $R_{factor} = R_{merge}$ for data collected from the image plate, where $R_{merge} = \sum_{all\ i}|\langle I\rangle - I_i|/\sum I_i$. [b] For data collected from the area detector, $R_{factor} = R_{sym}$, where $R_{sym} = \{[\sum_{hkl}\sum_{i=1}^{N} w_i(I_{av} - I_i)^2]/[\sum_{hkl}\sum_{i=1}^{N} w_i(I_i)^2]\}^{1/2}$, $I_{av} = 1/N\sum_{i=1}^{N} I_i$, and $w_i = 1/\sigma_i^2$.

Table 2: Crystallographic Refinement Statistics for TS−CF_3dUMP

total no. atoms	2681
total no. waters	48
Diffraction Agreement	
total unique reflections	15500
R_{factor}[a] (%)	21.3
Stereochemical Ideality	
bond lengths (Å)	0.018
bond angles (deg)	3.7
dihedrals (deg)	25.2
av B-factor (Å^2)	17

[a] $R_{factor} = \sum|F_{obs} - F_{calcd}|/\sum F_{calcd}$.

Structural Solution. The structure was deduced from difference Fourier $(F_o - F_c)\alpha_{calcd}$ maps, where F_c and α_{calcd} were derived from a highly refined, phosphate-bound *L. casei* TS structure with coordinates for the phosphate removed (Finer-Moore et al., 1993). The CF_3dUMP was buuilt into the initial $(F_o - F_c)\alpha_{calcd}$ map; in later $(F_o - F_c)\alpha_{calcd}$ maps the degradation product 5-carboxy-dUMP was modeled into additional electron density within the active site. The model was refined using the program XPLOR (Brünger et al., 1987) by alternating 40 cycles of energy minimization with 5 cycles of individual restrained B-factor optimization until it reached convergence. Additional waters were identified from $(F_o - F_c)\alpha_{calcd}$ maps, and after further refinement, the density for each was checked using omit maps. Crystallographic refinement statistics are given in Table 2.

Structural Comparison. Superposition of the TS−CF_3dUMP structure with the refined *L. casei* TS−dUMP structure was accomplished by aligning the two structures such that the rms deviation in the C_α positions was minimized (Kabsch, 1978) using the program GEM (Fauman, 1993).

RESULTS

UV/Visible Difference Spectra. Treatment of *L. casei* TS with CF_3dUMP in the absence of thiols led to the formation of a new chromophore absorbing between 290 and 340 nm, which was stable for at least 1 h (Figure 1). Spectral titration of a constant amount of CF_3dUMP (10 μM) with TS showed that the stoichiometry of the interaction was 1 CF_3dUMP per TS monomer (Figure 1, inset), giving a $\Delta\epsilon_{304}$ of 4600 M^{-1} cm^{-1} per monomer. Using 8.5 μM TS and 10 μM CF_3-

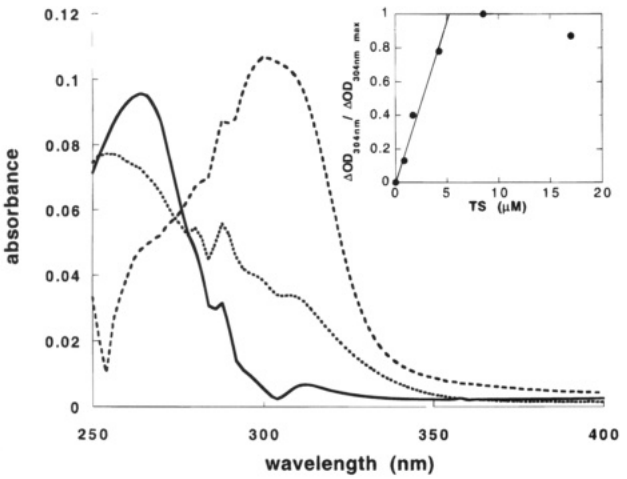

FIGURE 1: Difference spectra of a reaction mixture containing 8.5 μM TS and 10 μM CF_3dUMP in a total volume of 1 mL. Spectra were recorded immediately after the addition of CF_3dUMP (—) and after 310 s (•••). The final spectrum was stable for at least 1 h. The third spectrum (- - -) was recorded 30 min after the addition of 6 mM DTT to the reaction mixture and the reference. Inset: Spectral titration of CF_3dUMP with TS. The final concentration of CF_3dUMP was 10 μM (total volume, 1 mL in standard TES buffer). The ratios of absorbance changes with varying TS concentrations (ΔOD_{304nm}) to the maximal absorbance change ($\Delta OD_{304nm\ max}$) are plotted against TS concentrations.

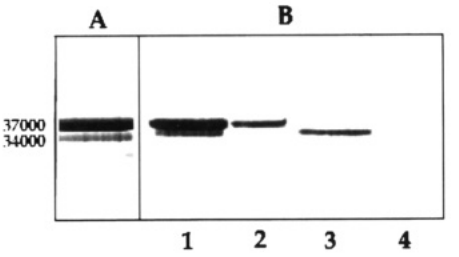

FIGURE 2: (A) Visualization of the enzyme−inhibitor complex on SDS−PAGE. The complex was formed by incubating TS with CF_3dUMP for 1 h. A new band with an apparent molecular weight of 34 000 appeared (unliganded TS migrates with an apparent MW of 37 000). (B) Degradation of the tritium-labeled complex in the presence of β-mercaptoethanol. Lane 1, SDS−PAGE of untreated complex; lane 2, SDS−PAGE of complex treated with β-mercaptoethanol; lanes 3 and 4, autoradiography of lanes 1 and 2.

Table 3: Measurement of Fluoride Ion Release in the Reaction of *L. casei* TS with CF_3dUMP[a]

	A	B	C[b]	D[c]
[TS monomer]	50 (1)	180 (3)	50 (1)	
[CF_3dUMP]	200 (4)	60 (1)	200 (2)	114 (1)
[F^-] released	100 (2)	120 (2)	150 (3)	350 (3)

[a] All concentrations are given in micromolar, followed in parentheses by the number of fluoride equivalents released. TS−CF_3dUMP reaction incubation times were 30 min. TISAB (4 mL) was added to all reactions prior to measurement. No fluoride release was detected in control reactions containing either TS or CF_3dUMP alone. [b] A 60 min reaction with 35 mM DTT followed TS−CF_3dUMP incubation. [c] Hydrolysis of CF_3dUMP at pH 13, 37 °C, in the absence of TS (72 h).

dUMP, the apparent first-order rate constant for the absorbance increase at 304 nm was 7.2×10^{-3} s^{-1} ($t_{1/2} \approx 96$ s).

Addition of β-mercaptoethanol or DTT to the preformed enzyme−inhibitor complex gave similar spectra that demonstrated a time-dependent increase of the absorbance between 290 and 340 nm and the appearance of a shoulder at 240 nm. In a reaction mixture containing 8.5 μM TS, 90 μM CF_3dUMP, and 6 mM β-mercaptoethanol, the absorbance at 304 nm increased rapidly within the first 10 min, followed by a slower increase that was complete after 3 h. When 3 mM DTT was used, the increase at 304 nm was complete after 30 min, and the end point was 7 times lower than that with β-mercaptoethanol; the final spectrum is shown in Figure 1.

Nitrocellulose Filter Binding and Gel Filtration. When TS was incubated with excess [2′-^{3}H]CF_3dUMP in the absence of thiols, the enzyme−inhibitor complex could be isolated on nitrocellulose filters. The complex formed with $k = 7.7 \times 10^{-3}$ s^{-1} ($t_{1/2} \approx 90$ s) and was stable for at least 2 h. The presence or addition of DTT to the preformed TS−[2′-^{3}H]CF_3dUMP complex resulted in the slow release of the label from the protein (data not shown), with $k = 1.8 \times 10^{-5}$ s^{-1} ($t_{1/2} \approx 650$ min).

A preformed complex of TS−CF_3dUMP treated with DTT was either diluted in assay buffer and assayed directly or filtered through Sephadex G-25 to remove free ligand prior to assay. Without gel filtration, TS activity was undetectable for as long as 8 h; however, when gel filtration was used to remove small molecules, there was a slow recovery of activity (ca. 60% in 8 h).

SDS−PAGE. In the absence of thiols, the TS-[2′-^{3}H]CF_3-dUMP complex can be isolated on SDS−PAGE (Figure 2A). When 10 μM TS was incubated with 10 μM [2′-^{3}H]CF_3-dUMP, two protein bands, corresponding to 34 and 37 kDa, were observed on SDS−PAGE. The 37 kDa band corresponded to unmodified TS and was about 5-fold more intense than the 34 kDa band. Autoradiography showed that the radioactive label was present only in the 34 kDa band (Figure 2B, lanes 1 and 3). When the preformed complex was boiled in loading buffer containing 50 mM β-mercaptoethanol before application to the gel, the intensity of the 34 kDa band became weaker and finally disappeared (Figure 2B, lanes 2 and 4).

Inhibition of TS Activity. Incubation of 8.5 μM TS with 50 μM CF_3dUMP resulted in time-dependent loss of TS activity with $k = 7.7 \times 10^{-3}$ s^{-1} ($t_{1/2} \approx 90$ s), similar to the time course of the spectral change at 304 nm and formation of the complex isolable on nitrocellulose filters.

Fluoride Release. ^{19}F NMR and a fluoride-specific electrode were used to show that treatment of CF_3dUMP with TS in the absence of thiols results in the release of fluoride ions. In ^{19}F NMR, free CF_3dUMP showed one sharp singlet signal with a chemical shift of −67 ppm, relative to $CFCl_3$. Upon addition of TS, this signal disappeared and a new signal at −124 ppm was observed, characteristic of free fluoride ions (Sohar, 1984). Addition of NaF to this mixture increased the intensity of this peak.

The release of fluoride from CF_3dUMP was quantitatively monitored with a fluoride-sensitive electrode. In the absence of thiols, and using either limiting TS (Table 3, column A) or limiting CF_3dUMP (Table 3, column B), 2 equiv of fluoride was released for every TS−CF_3dUMP complex formed, leaving one fluorine atom in the complex. When DTT was added to the complex, an additional equivalent of fluoride was released within 20 min (Table 3, column C).

Identification of a Covalently Modified Peptide Fragment. The TS−[2′-^{3}H]CF_3dUMP complex formed in the absence

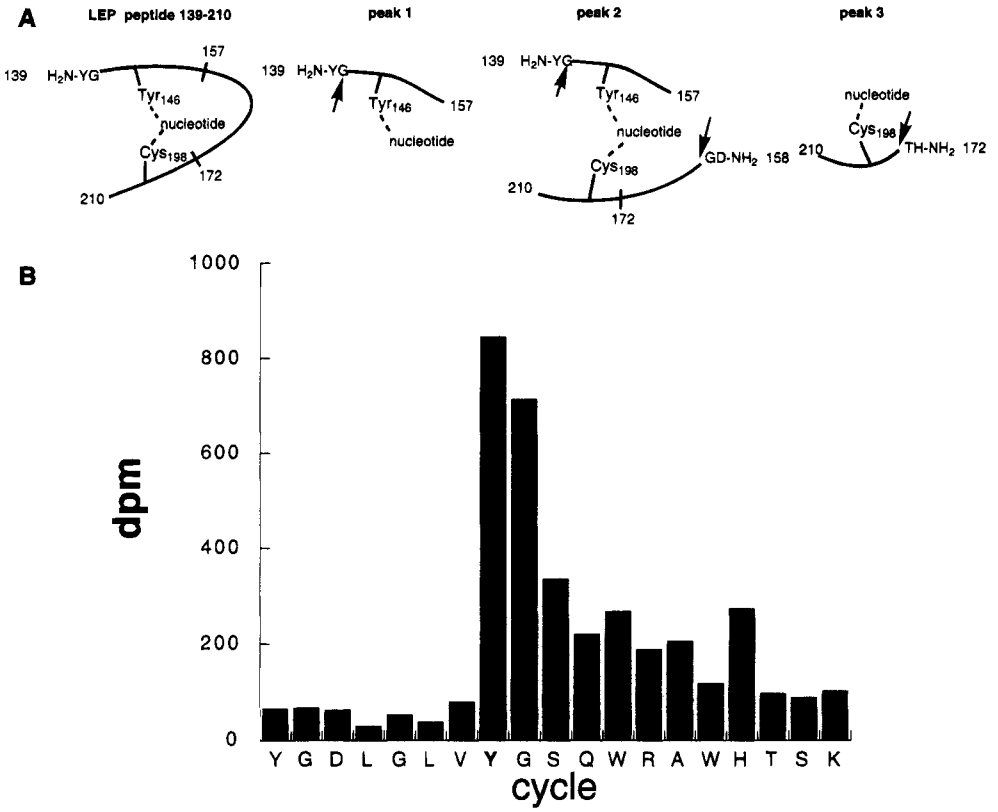

FIGURE 3: (A) Cartoon depicting radiolabeled peptides from LEP digestion of the TS−CF_3dUMP complex isolated by HPLC. Arrows indicate N-termini found in amino acid sequencing. (B) Peptide sequencing of tritium-labeled LEP digestion peptide 1 by gas-phase Edman degradation. Phenylthiohydantoin fractions were collected and counted in a liquid scintillation counter.

of thiols was digested with LEP, and the products were separated by HPLC and collected. Radioactivity wasrecovered in three separate peaks, which were subjected to N-terminal sequencing. The first peak contained 70% of the label and had the N-terminal sequence YGDLG, corresponding to LEP peptide 139−157 of TS (Figure 3). Mass spectroscopy showed a peptide of 2224.99 Da, in agreement with the theoretical value of 2224.09 Da for LEP peptide 139−157. The expected CF_3dUMP-modified peptide was not detected, indicating that the bound nucleotide was unstable under the conditions of mass spectral analysis. The peptide was sequenced in its entirety, with the collection of each phenylthiohydantoin product for quantitation of radioactivity. As shown in figure 3, the major peak of radioactivity was released in the cycle corresponding to Tyr 146. The second and third HPLC peaks each contained about 15% of the radioactivity found in the first peak. The second peak contained the N-terminal sequences YGDLG and GDTID, corresponding to LEP peptides 139−157 and 158−172, respectively. The third peak had the N-terminal sequence THPYS, corresponding to LEP peptide 173−210, which contains Cys 198. Neither the second nor the third HPLC peak was submitted for mass spectral analysis due to the relatively low amount of radioactive label detected in either peak and the unstable nature of the bound nucleotide.

These data may be explained as follows (Figure 3). LEP digestion generated three CF_3dUMP-bound peptides emanating from residues 139−210 by cleavages at residues 158 and 173. The first peptide contains residues 139−157, with the nucleotide covalently bound to Tyr 146. The second peptide contains an incomplete digestion product, which contains residues 139−157 and residues 158−210, cross-linked by covalent linkages to the nucleotide *via* Tyr 146 and Cys 198. Alternatively, the free LEP peptide 158−172 coeluted in the second peak with the LEP peptide 139−157−CF_3dUMP adduct. The third peptide contains residues 173−210 and has the nucleotide covalently linked to Cys 198.

Isolation of Reaction Products. Two different procedures were employed for the isolation of the reaction products resulting from the incubation of TS, CF_3dUMP, and DTT. Application of the reaction mixture to paper chromatography yielded two major reaction products. The first product (λ_{max} = 268 nm at pH 6 and pH 13; λ_{min} = 238 nm at pH 6 and 246 nm at pH 13) was unstable in 0.1 N HCl and converted into the second product. The second product (λ_{max} = 275 nm at pH 6 and 273 nm at pH 13; λ_{min} = 243 nm at pH 6 and 241 nm at pH 13) was stable in acid, but degraded into 5-carboxy-dUMP when treated with NaOH. Both products exhibited absorbance maxima that were shifted toward longer wavelengths, indicating a change in substitution at C_5 (Mason, 1962).

A mixture of reaction products with UV/vis spectra similar to those of the products isolated by paper chromatography was also isolated using reverse-phase HPLC. Electrospray mass spectroscopy of the HPLC-purified product pool yielded signals for mass to charge ratios of 471.2 and 663.2, in accord with proposed structures **VI** and **VIa** (Figure 4). There were also associated signals with 38 Da mass differences attributed to the complexation of nucleotides with potassium ions, similar to that seen in the spectra of synthetic oligonucleotides containing sodium adducts (Stults & Marsters, 1991).

Crystal Structure of TS−CF_3dUMP Complex. Hexagonal bipyramidal crystals grew in 1 week at room temperature to average dimensions of 0.7 × 0.3 × 0.3 mm. The space

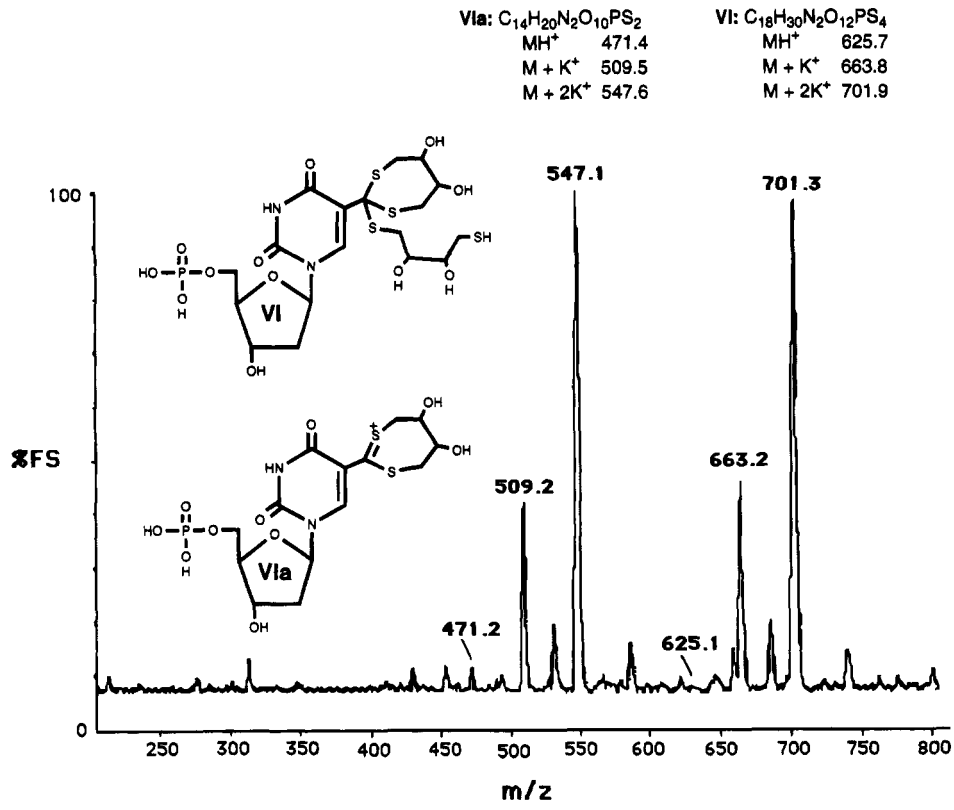

FIGURE 4: Electrospray mass spectrum and proposed chemical structures for isolated reaction products from the degradation of enzyme–inhibitor complex by DTT.

group was $P6_122$, with unit cell dimensions of $a = b = 78.4$ Å and $c = 242.2$ Å, similar to those determined for previous *L. casei* TS structures (Finer-Moore et al., 1993; Hardy et al., 1987). The initial difference Fourier maps using either the 2.3 Å image plate data or the 2.8 Å area detector data against the phosphate-bound *L. casei* TS structure gave similar results, and both clearly indicated density in the active site for CF_3dUMP (Figure 5). The *R*-factor between these two data sets was 6% on amplitudes after Wilson scaling, and a difference map calculated using the terms $(F_1 = F_2)\alpha_{calcd}$, where F_1 and F_2 are the amplitudes from the two scaled data sets, was featureless. Therefore, the image plate and area detector data were merged for structural refinement.

Positioning CF_3dUMP into the difference density put C_7 of the pyrimidine within 1.5 Å of the hydroxyl group of Tyr 146, indicating covalent attachment (Figure 5). The electron density indicated a nearly tetrahedral arrangement of atoms about C_7, suggesting the attachment of a substituent in addition to Tyr 146; **IIIa** shows a hypothetical structure where water has added to C_7 and enzyme has been eliminated from **III**. However, the close proximity of C_6 to the Cys 198 sulfur (3.0 Å) and the absence of electron density for C_6 suggested that the crystal may be a mixture of species **III**, where C_6 is covalently bound to the active site sulfhydryl, and a structure like **IIIa**, where it is not. Refinement of either species gave the same *R*-factor ±0.2% and left the pyrimidine ring centered in the original difference density shown in Figure 5.

Comparison of the refined TS–CF_3dUMP and TS–dUMP binary complexes indicates that the protein structures are nearly identical, with rms deviations within 0.5 Å for superimposed C_α positions. While the phosphate group of CF_3dUMP occupies the same position as the phosphate of dUMP in the TS–dUMP structure, the most significant difference between the two structures is in the relative positions of the pyrimidine and ribose. A 30° change in the glycosidic bond torsion angle χ ($\chi = 160°$ for CF_3dUMP and $\chi = -168°$ for dUMP; Saenger, 1984) is seen for CF_3-dUMP relative to dUMP, although both nucleotides are bound in the *anti* conformation (Saenger, 1984; Finer-Moore et al., 1993). Furthermore, both dihedral angles β and γ (P–O5′–C5′–C4′ and O5′–C5′–C4′–C3′, respectively; Saenger, 1984) for CF_3dUMP differ by 120° from the same angles in the dUMP structure. The cumulative effect of these differences is an apparent translation of 3.2 Å and a rotation of nearly 85° by CF_3dUMP toward Tyr 146 about an axis connecting the atoms O4 of the pyrimidine and P of the phosphate of CF_3dUMP (Figure 5). The hydrogen bond from the ribose 3′-hydroxyl to the Tyr 261 hydroxyl observed in the TS–dUMP structure has been disrupted and replaced by an intervening water molecule. Arg 23, which is disordered in the *L. casei* phosphate-bound structure, shifts by nearly 2 Å to interact with both the CF_3dUMP ribose hydroxyl and the phosphate. All water molecules identified in the CF_3dUMP structure are also present in the dUMP binary complex, except that the water that has been proposed to discriminate between substrate and product (Fauman et al., 1994) has been replaced by the C_7 atom of CF_3dUMP.

Electron density corresponding to the degradation product 5-carboxy-dUMP (**VII** in Scheme 2) was also observed in initial difference Fourier maps, and this ligand was refined separately (data not shown). While there is overlap for the phosphate moiety of CF_3dUMP and 5-carboxy-dUMP, the density for 5-carboxy-dUMP does not allow covalent attachment to the enzyme.

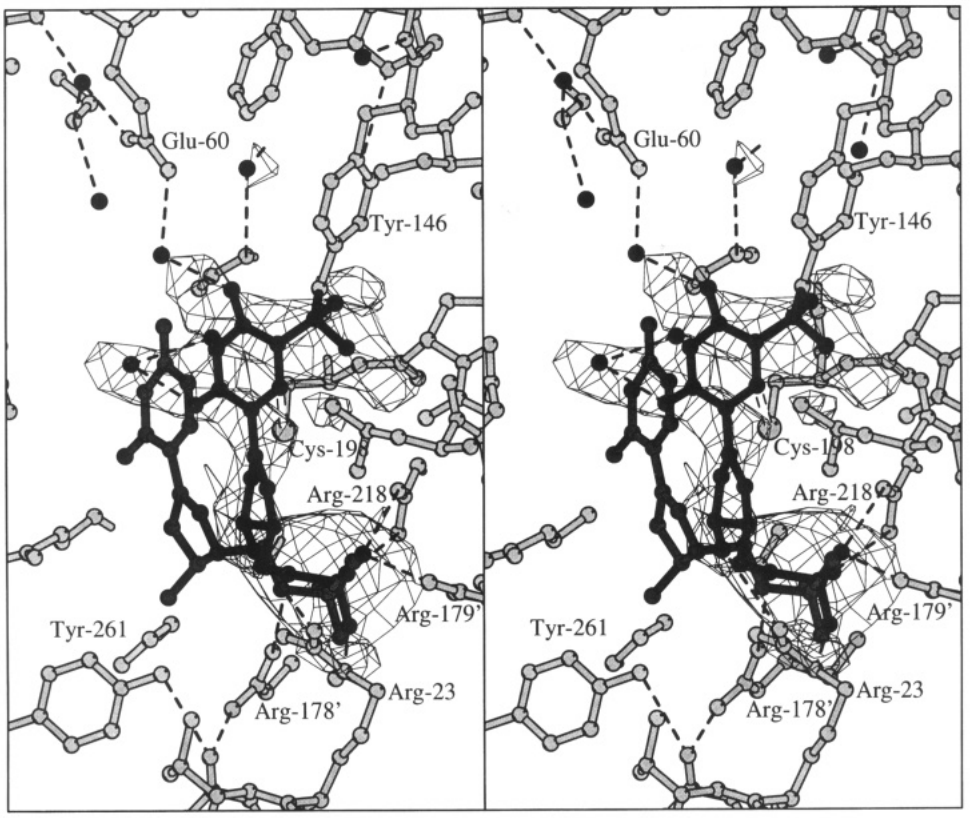

FIGURE 5: Stereoview of the original omit $F_o - F_c$ map for CF_3dUMP (black), clearly revealing a covalent attachment to Tyr 146. The superposition of dUMP (gray) demonstrates the change in position of the nucleotide within the active site to allow interaction with Tyr 146.

Scheme 2

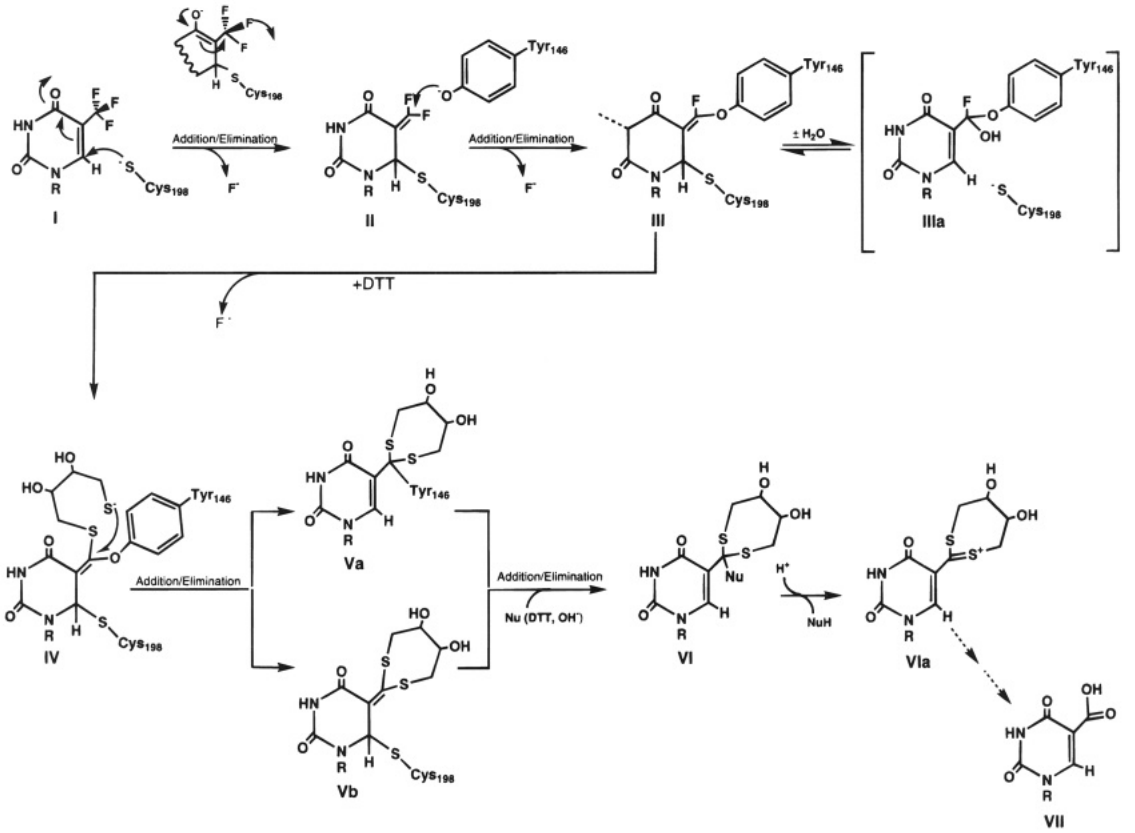

DISCUSSION

Scheme 2 shows a proposed mechanism for the interaction of TS with CF_3dUMP. After reversible binding of CF_3dUMP to the active site, the thiol of Cys 198 attacks C_6 of nucleotide **I**, causing the expulsion of a fluoride ion from C_7 and the formation of the reactive exocyclic difluoromethylene intermediate **II**. Subsequently, the electrophilic C_7 of **II** reacts with the hydroxyl group of Tyr 146, resulting in the release

of a second fluoride ion and the formation of covalent complex **III**. In this complex, TS is cross-linked between Cys 198 and Tyr 146 by the inhibitor.

The evidence that supports the conversion of **I** to **III** is as follows. (i) Formation of a covalent TS−nucleotide complex was demonstrated by the inactivation of TS by CF_3dUMP and the isolation of a TS−nucleotide complex using nitrocellulose filtration, gel filtration, or SDS−PAGE under nonreducing conditions. (ii) The UV/vis spectral changes and the release of two fluoride ions demonstrate modification of CF_3dUMP at C_5 (Mason, 1962) and are in accord with the conversion of **I** to **III**. The necessity for nucleophilic attack at C_6 to activate the 5-CF_3 group of CF_3dUMP for such transformations is well established (Santi & Sakai, 1971; Wataya et al., 1987). (iii) The time courses of enzyme inactivation, binding to nitrocellulose filters, changes in the UV/vis spectra, and fluoride release were similar, suggesting that all experiments monitor the same process (i.e., conversion of **I** to **III**). (iv) Nonreducing SDS−PAGE showed the TS−CF_3dUMP complex migrating faster than TS (MW 34 000 versus 37 000); the complex could be dissociated and TS regenerated by treatment with thiols. Cross-linking of proteins, as proposed for **III**, can lead to smaller hydrodynamic volumes and enhanced motility on SDS−PAGE (Pollitt & Zalkin, 1983). (v) Sequencing of peptides isolated from LEP digestion of the complex unambiguously identified Tyr 146 as the site of covalent attachment of the inhibitor.

The refined crystal structure, with a final *R*-factor of 20% and excellent geometry, verified the covalent attachment of the inhibitor to the enzyme at Tyr 146. The covalently bound CF_3dUMP is tethered to the dUMP binding site by its phosphate group (Finer-Moore et al., 1993), but the pyrimidine and ribose groups occupy different positions compared to the TS−dUMP binary complex. Combined changes in CF_3dUMP dihedral angles χ, β, and γ give a net 3 Å shift and 90° rotation for CF_3dUMP with respect to the position of dUMP in the TS−dUMP structure. This shift in position allows CF_3dUMP to interact with Tyr 146 while simultaneously displacing a conserved water molecule adjacent to C_5. The hydrogen bond from the ribose 3′-hydroxyl to the Tyr 261 hydroxyl has been replaced by an intervening water molecule, and Arg 23 shifts by 2 Å relative to its position in the TS-P_i structure to coordinate both the ribose hydroxyl and the phosphate groups of CF_3dUMP. Species **III** seems to be present in the crystal structure, but it is accompanied by a species in which C_7 is nearly tetrahedral and which does not have the electron density expected of a covalent linke to C_6. Refinement of the complex with or without a covalent bond between C_6 and the Cys 198 sulfur (species **III** and **IIIa**) yielded the same *R*-factor and similar $2F_o - F_c$ difference density. The weak electron density between these two atoms probably resulted from a mixture within the crystal of covalently and noncovalently bound species. To explain this, we suggest that a water molecule may reversibly add to C_7 of **III** with concomitant cleavage of the bond to Cys 198 to form species **IIIa**. We recongize that this should be unstable in solution; however, it could be stabilized by the enzyme, and it accommodates the structural and biochemical data.

The remainder of the mechanism was deduced from studies of the treatment of the preformed complex with thiols. As shown in Scheme 2, it is proposed that a thiol group adds to C_7 of **III** to eliminate the third fluoride ion from the complex and form **IV**. The addition of a second thiol group[2] of DTT to C_7 of **IV** would eliminate Tyr 146 to give **V**. Finally, nucleophilic attack of another thiol or a water molecule at C_7 of **V** would liberate nucleotide **VI**.

The mechanism in Scheme 2 is supported by the following experimenal findings. (i) Treatment of the enzyme−inhibitor complex with thiols resulted in changes in the UV/vis spectrum and release of the third fluoride ion from the complex. These results are consistent with conversion of the enzyme−inhibitor complex **III** to an intermediate(s) where the fluoride of **III** is replaced by thiol (**IV** and **V**, Scheme 2). (ii) Thiol treatment also resulted in slow destruction of the covalent complex and formation of a tightly bound noncovalent complex **VI**. Destruction of the covalent bond was shown using nitrocellulose filtration, gel filtration, and nonreducing SDS−PAGE; the formation of a tightly bound noncovalent complex was indicated by the requirement of gel filtration to restore enzyme activity. (iii) Finally, we isolated two reaction products from the reaction of the enzyme−inhibitor complex with DTT, and their masses agreed with those of the proposed structures **VI** and **VIa** (Figure 4 and Scheme 2). The predicted chemical stability of these products in acid or base is compatible with that of the proposed structures **VI** and **VIa**; however, we could not find analogous structures in the reported literature and cannot cite precedent for the proposed properties. Protonation of a sulfur in **VI** would release DTT and result in **VIa**, which should be stable in acids. It is also reasonable to suggest that hydroxide would eventually degrade **VIa**, but not **VI**, by addition−elimination reactions to give the observed 5-carboxy-dUMP.

When modeled into the nucleotide binding site of TS, the CF_2 group of **II** is rigidly held some 3.5 Å away from the Tyr 146 hydroxyl; one would not normally predict that these two groups would react. The fact that a covalent bond is formed is an indication of the conformational flexibility of the protein or the ligand within the active site. Indeed, when Tyr 146 reacts with the C_7 of CF_3dUMP, the pyrimidine is displaced from its binding site and the covalent complex relaxes to the structure dictated by the new covalent bond. This indicates that a reactive electrophile, generated from a mechanism-based inhibitor, and the enzyme nucleophile with which it reacts need not initially be in perfect proximity for covalently bond formation. Indeed, *trans*-5-(3,3,3-trifluoro-1-propenyl)-2′-deoxyuridylate is also a potent inhibitor of TS (Wataya et al., 1979), although the CF_3 moiety must be projected quite differently in the active site than it is in the TS−CF_3dUMP structure. It may be speculated that even more effective inhibitors of TS might be obtained by structure-guided design of CF_3dUMP analogs that better position the reactive group with respect to Tyr 146. In a broader context, certain mechanism-based inhibitors may not require as stringent juxtaposition of reactive groups as generally believed. If correct, this would expand the number of potential reactive nucleophiles in target proteins and allow considerably more flexibility in the design of mechanism-based enzyme inhibitors.

[2] The mechanism shows the reaction with DTT; with 2-mercaptoethanol, the intramolecular reaction would be depicted as an intermolecular reaction with another molecule of 2-mercaptoethanol.

ACKNOWLEDGMENT

We thank Chris Carreras and Jim Kealey for helpful discussions and reading of the manuscript and Robert M. Stroud for suggestions regarding structural interpretation. Data collection at the UCSF Mass Spectroscopy Facility was funded by the Biomedical Research Technology Program of the National Center for Research Resources (NIH NCRR BRTP 01614).

REFERENCES

Bradford, M. M. (1976) *Anal. Biochem. 72*, 248−254.
Bruice, T. W., & Santi, D. V. (1982) *Biochemistry 21*, 6703−6709.
Brünger, A. T., Kuriyan, J., & Karplus, M. (1987) *Science 235*, 459.
Carmine, A. A., Brogden, R. N., Heel, R. C., Speight, T. M., & Avery, G. S. (1982) *Drugs 23*, 329−353.
Chamberlain, J. P. (1979) *Anal. Biochem. 98*, 132−135.
Fauman, E. B. (1993) Ph.D. Thesis, University of California, San Francisco.
Fauman, E. B., Rutenber, E. E., Maley, G. F., Maley, F., & Stroud, R. M. (1994) *Biochemistry 33*, 1502−1511.
Ferrin, T. E. (1988) *J. Mol. Graphics 6*, 13−27.
Finer-Moore, J., Fauman, E. B., Foster, P. G., Perry, K. M., Santi, D. V., & Stroud, R. M. (1993) *J. Mol. Biol. 232*, 1101−1116.
Greene, P. J., Maley, F., Pedersen-Lane, J., & Santi, D. V. (1993) *Biochemistry 32*, 10283−10288.
Hardy, L. W., Finer-Moore, J. S., Montfort, W. R., Jones, M. O., Santi, D. V., & Stroud, R. M. (1987) *Science 235*, 448−455.
Heidelberger, C., & King, D. H. (1979) *Pharmacol. Ther. 6*, 427−442.
Heidelberger, C., Boohar, J., & Kampschroer, B. (1965) *Cancer Res. 25*, 377−381.
Higashi, T. (1990) *J. Appl. Crystallogr. 23*, 253−257.
Kabsch, W. (1978) *Acta Crystallogr. A34*, 827−828.
Kabsch, W. (1982) *J. Appl. Crystallogr. 15*, 916−924.
Kealey, J. T., & Santi, D. V. (1991) *Biochemistry 30*, 9724−9728.
Kealey, J. T., & Santi, D. V. (1992) *Protein Expression Purif. 3*, 380−385.
Laemmli, U. K. (1970) *Nature 27*, 680−685.
Mason, S. F. (1962) *Heterocycl. Comp. 16*, 477−493.
Pogolotti, A. L. J., Danenberg, P. V., & Santi, D. V. (1986) *J. Med. Chem. 29*, 478−482.
Pollitt, S., & Zalkin, H. (1983) *J. Bacteriol. 153*, 27−32.
Prasher, D. C., Carr, M. C., Ives, D. H., Tsai, T.-C., & Frey, P. A. (1982) *J. Biol. Chem. 9*, 4931−4939.
Reyes, P., & Heidelberger, C. (1965) *Mol. Pharmacol. 1*, 14−30.
Saenger, W. (1984) in *Principles of Nucleic Acid Structure*, pp 17−24, Springer-Verlag, New York.
Sakai, T. T., & Santi, D. V. (1973) *J. Med. Chem. 16*, 1079.
Santi, D. V., & Sakai, T. T. (1971) *Biochemistry 10*, 3598−3607.
Sato, M., Yamamoto, M., Imada, K., Katsube, Y., Tanaka, N., & Higashi, T. (1992) *J. Appl. Crystallogr. 25*, 348−357.
Sohar, P. (1984) *Nuclear Magnetic Resonance Spectroscopy*, CRC Press, Boca Raton, FL.
Stults, J. T., & Marsters, J. C. (1991) *Rapid Commun. Mass Spectrom. 5*, 359−363.
Umeda, M., & Heidelberger, C. (1968) *Cancer Res. 28*, 2529−2538.
Wataya, Y., Matsuda, A., Bergstrom, D. E., Ruth, J. L., & Santi, D. V. (1979) *J. Med. Chem. 22*, 339−340.
Wataya, Y., Sonobe, Y., Maeda, M., Yamaizumi, Z., Aida, M., & Santi, D. V. (1987) *J. Chem. Soc., Perkin Trans 1*, 2141−2147.